Interferometric Synthetic Aperture Sonar

S. Banks, T. Sutton, H.Griffiths

University College London

Abstract: *Interferometric Synthetic Aperture Sonar (ISAS) offers the possibility of high resolution, three-dimensional images of objects on the ocean floor. The height of objects is identified from the phase difference between two synthetic aperture images of the object obtained using two receivers separated by a short distance. A central problem is the need to unwrap the phase difference in the presence of noise to obtain an unambiguous height estimate.*

This paper presents an end-to-end simulation of ISAS processing algorithms. The algorithms presented have been shown to work on real sonar data also.

1 Introduction.

Interferometric sonar may be used to obtain three dimensional images of the ocean floor, or targets on the ocean floor. Interferometry has been used successfully by the radar community for a number of years, however its application to sonar has developed more slowly due to a number of factors such as increased platform motion an noise. Nonetheless, a small number of working, although mostly experimental, ISAS systems exist including the Kiwi SAS [1], DARPA SAS [2] and the DERA SAS. The DERA SAS, used for this project, is a rail mounted system hence motion errors are very small. The work described in this paper has been carried out as part of a collaboration between DERA, Thompson Marconi Sonar, EPSRC and UCL to develop a high resolution synthetic aperture sonar system.

2 The Interferometric Synthetic Aperture Sonar Process

The ISAS process divides easily into two parts (1) The creation of two synthetic aperture sonar images, (2) processing these images to obtain height estimation. A description of both processes follows, however this paper will concentrate on the latter – the creation of a 3D image.

2.1 Synthetic Aperture Processing

Synthetic aperture processing allows a high resolution image to be formed by combining many sets of data obtained using a small receiver at different locations. Such techniques are common in radio astronomy and radar also. The system described in this paper uses a vernier receiving array (several elements) moving along a straight track, *Figure 1*. The azimthual resolution of such a system can be shown to be independent of range, and equal to half the length of the real aperture [3]. Several image reconstruction algorithms exist, the *chirp scaling algorithm* was used here [4].

2.2 Interferometric Height Estimation

The height of a target scene may be estimated from the phase difference between two images of the target scene taken from spaced receivers [6]. The geometry is shown in *Figure 1.*

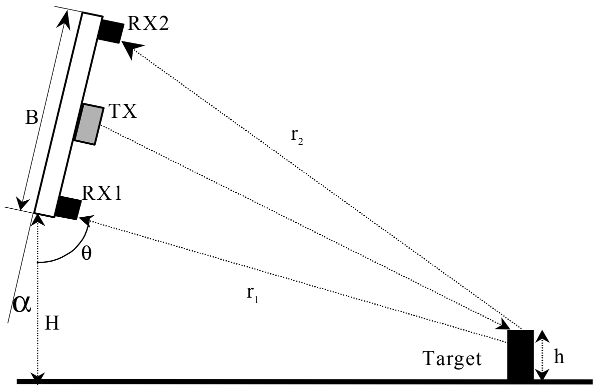

Figure 1 Simulated Geometry

The process is complicated by *phase ambiguity,* i.e. when the phase difference between the two received signals is greater than 2π radians. Phase ambiguity may be removed by *phase unwrapping*, discussed later.

The relative height of the target scene can be calculated from the unwrapped phase difference between the upper and lower images using **eqn 1,** where ϕ is the phase difference between the received signals at RX2 and RX1 and λ is the wavelength of the emitted chirp.

$$h = H - r_1 \cos\theta \quad \text{where: } \theta = \cos^{-1}\left(\frac{r_2^{\,2} - B^2 - r_1^{\,2}}{2 * B * r_1}\right) - \alpha \quad \text{and} \quad r_2 = r_1 + \frac{\phi\lambda}{2\pi} \qquad \textbf{eqn 1}$$

eqn 1 assumes the two images are perfectly co-registered. This will not be the case initially, hence before height estimation can take place the images must be co-registered.

2.3 Co-registration of two images

Co-registration of the two images is performed in two stages. The first stage is a correction based on the a-priori knowledge of the scene geometry, *Figure 1* (the target scene is assumed flat). Correction is carried out by moving pixels in the image formed from RX2 using an equation for the difference *(r2-r1)* as a function of *r1*, **eqn 2**.

$$(r_2 - r_1) = \sqrt{R + \left(\sqrt{(r_1^{\,2} - H^2)} - S\right)^2} - r_1 \quad \text{where: } S = B * \sin\alpha \;,\; R = (H + B * \cos\alpha)^2 \qquad \textbf{eqn 2}$$

Pixels must be co-registered to a sub pixel level; this is achieved by upsampling one image by a factor of 10. Pixels can then be selected from the up-sampled image that correspond to pixels in the second, non upsampled image.

The second co-registration stage involves performing a cross-correlation between small areas of the upper and lower images. Selected areas of the up-sampled image are shifted by an amount corresponding to a peak in the cross correlation coefficient between the two images.

3 Results using simulated data

Software has been written to simulate the sonar reflections off a given target scene. The simulation represents the scene using a finite number of point reflectors spaced at a distance equivalent to the resolution of the SAS image processing. Closer spacing results in a *smooth* reflective surface, which is hard to detect using sonar as most of the reflected signal is reflected away from the receiver.

Figure 2 shows two images obtained for a simulated Gaussian mound, along with the resulting interferogram. The colour of the image represents phase, the brightness amplitude. The interferogram shows the difference in phase between the two co-registered SAS images and the sum of the magnitudes.

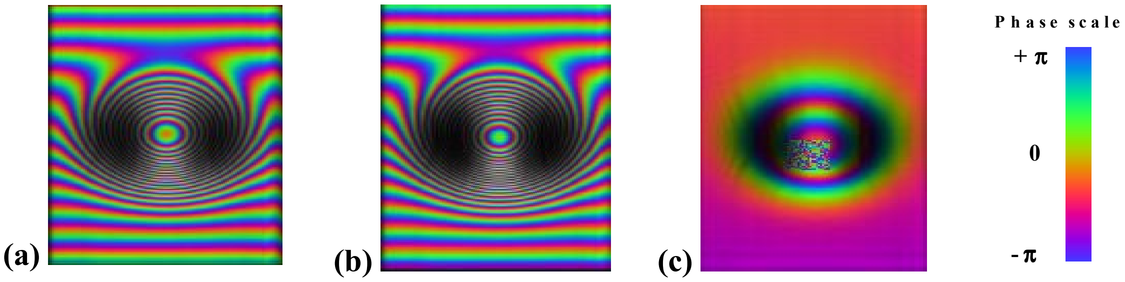

Figure 2 (a) Phase of image produced from upper receiver, (b) phase of image produced by lower receiver, (c) interferogram i.e. the phase difference between (a) and (b)

3.1 Phase unwrapping

The phase in the interferogram in modulo 2π; this must be *phase-unwrapped* to obtain the true phase. Several phase unwrapping techniques exist; the technique described below was first proposed in [5]. *Figure 3* shows an example normalised phase map. The true phase is assumed to change no more than 0.5 between pixels; there is therefore a corresponding maximum gradient assumed for the target scene. Phase unwrapping starts from a chosen pixel. A path from this pixel is chosen that covers the whole interferogram. Moving along the path, if magnitude of the difference between the current and next pixel is greater than 0.5, 1.0 is either added or subtracted from the next pixel as appropriate such that the magnitude of the phase difference is less than 0.5.

0.1		0.2		0.5		0.3
	0		*0*		*0*	
0.0	→	0.3		0.4	→	0.0
↑	*+1*	↓	*0*	↑	*-1*	↓
0.8	←	0.6		0.4	←	0.8
	0		*0*		*0*	
0.8		0.7		0.7		0.8

Figure 3 Positive and negative residues

Phase noise, layover or cliffs may cause areas in the interferogram where the phase cannot be easily unambiguously unwrapped; such areas may result in two different phase unwrapping paths to result in two different phase values for a given pixel. This situation may be avoided by identifying residues in the phase map. A residue is identified by phase unwrapping around a closed 4 pixel square. If this results in a change of the phase value of the first pixel of +1, the pixels are marked as a +ve residue; likewise a -ve residue if a phase change of -1 occurs.

All residues on the interferogram are identified. Residues are paired with the a near residue of the opposite sign, or a pixel at the edge of the image, which ever is closer. Paired residues are linked using a 'cut line'.

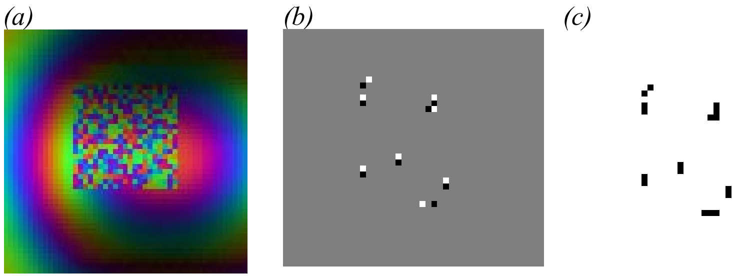

Figure 4 (a) Noisy part of interferogram, (b) residues: white = -1, black = +1, (c) linked residues

For the simulation, residues have been generated by adding 3.2 rad peak noise to a small area of the interferogram, *Figure 4***.** It is desireable to minimise the total length of the cut lines, especially when the residue density is high. For low residue densities, the *nearest neighbour algorithm* [5] works well, however fails to find an optimum solution in areas of high residue density. An improved algorithm based on *simulated annealing* has been developed as part of this work that can always find a solution close to the optimum solution. The 'quality' of the solution can be varied at the expense of computation time.

3.2 Filtering

The number of residues in an interferogram may be reduced by applying filtering, although this reduces the resolution of the image also. Using a real data set, the number of residues was reduced from 40,000 to 15,000 by forming a new filtered interferogram, $\boldsymbol{I_{filt}}$ where each pixel is set to a value given by **eqn 3.**

$$I_{filt}(p,q)=\frac{1}{2}\sum_{x=1}^{x=3}\sum_{y=1}^{y=3}I(p-2+x,q-2+y)*Filt(x,y)$$

Where $\boldsymbol{I}$ is the original interferogram,

$$\boldsymbol{Filt}=\begin{bmatrix}0.125 & 0.125 & 0.125\\ 0.125 & 1.0 & 0.125\\ 0.125 & 0.125 & 0.125\end{bmatrix}$$

eqn 3

3.3 Scene height calculated from phase-unwrapped interferogram

Figure 5b shows the image from data phase unwrapped in the right to left direction only, ignoring the cut lines. The diagram shows how errors resulting from unwrapping past a cut line are propagated across the image. *Figure 5a* shows the same data phase unwrapped using a path that does not cross the cut lines.

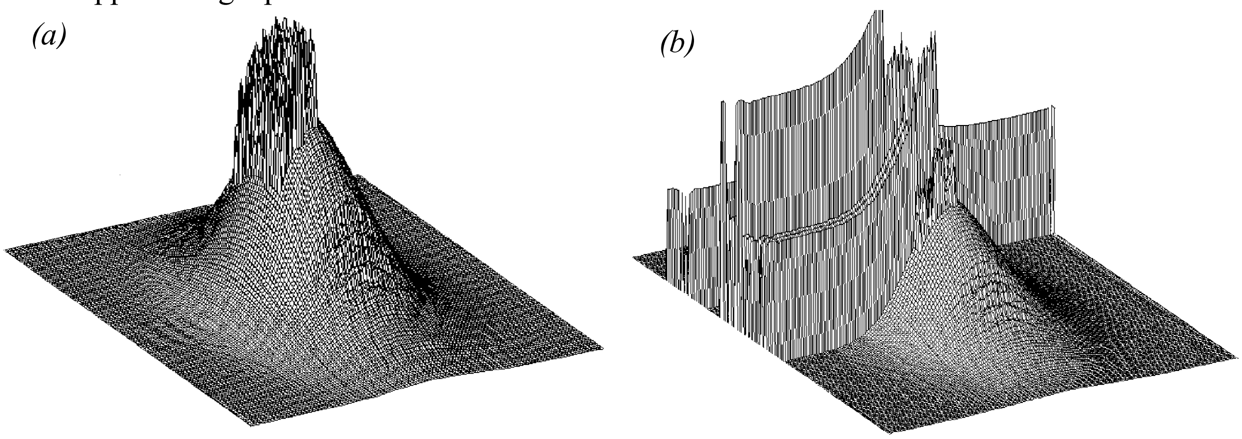

Figure 5(a) Reconstructed 3D image with noise (b) Errors propagated globally when cut lines are ignored

4 Conclusions

This paper has presented a set of ISAS processing algorithms that have been shown to work on simulated data and, in work not presented here, on real data provided by DERA. The algorithms provide a good basis on which to develop ISAS based target recognition and seabed topography mapping techniques. Future work will concentrate on improving the algorithms and developing methods of motion error compensation suitable for use with non rail mounted (e.g. towed body) SAS systems.

References

[1] http://www.elec.canterbury.ac.nz/research/sonar/SAS_history.htm

[2] **M.A. Nelson**, DARPA Synthetic Aperture Sonar, *Proceedings of the Adaptive Sensor Array Processing (ASAP) Workshop*, vol.1, pp 141-155, 15May 1998

[3] **Walter G. Carrara, Ron S. Goodman, Ronald M. Majewski**, *Spotlight Synthetic Aperture Radar Signal Processing Algorithms,* ,Artech House INC, pp 58-p163,1995

[4] **R. Keith Raney, H. Runge, Richard Balmer, Ian G. Cumming, Frank H. Wong**, Precision SAR Processing Using Chirp Scaling, *IEEE Transactions on Geoscience and remote sensing*, volume 32 (4), July 1994.

[5] **Richard M. Goldstein, Howard A. Zebker, Charles L. Werner**, Satellite Radar Interferometry: Two-dimensional Phase Unwrapping, *Radio Science*, volume 23 (4), pp 713-720, July-August 1988

[6] **Hugh Griffiths,** Interferometric synthetic aperture radar, *Electronics & Communication Engineering Journal*, December 1995